arXiv:1902.06553v2 [q-bio.NC] 19 Feb 2019

A computational model for grid maps in neural populations

Fabio Anselmi[1,2,*], Benedetta Franceschiello[3,4], Micah M. Murray[3-6], Lorenzo Rosasco[1,2]

1 Center for Brains, Minds, and Machines, MIT, Cambridge, MA, USA
2 Laboratory for Computational and Statistical Learning (LCSL) and IIT, Genova, Italy
3 The LINE (Laboratory for Investigative Neurophysiology), Department of Radiology, University Hospital Center and University of Lausanne, Lausanne, Switzerland
4 Ophthalmology Department, Fondation Asile des Aveugles and University of Lausanne, Lausanne, Switzerland
5 EEG Brain Mapping Core, Center for Biomedical Imaging (CIBM), Lausanne, Switzerland
6 Department of Hearing and Speech Sciences, Vanderbilt University, Nashville, TN, USA

* anselmi@mit.edu

Abstract

Grid cells in the entorhinal cortex, together with place, speed and border cells, are major contributors to the organization of spatial representations in the brain. In this contribution we introduce a novel theoretical and algorithmic framework able to explain the emergence of hexagonal grid-like response patterns from the statistics of the input stimuli. We show that this pattern is a result of minimal variance encoding of neurons. The novelty lies into the formulation of the encoding problem through the modern Frame Theory language, specifically that of equiangular Frames, providing new insights about the optimality of hexagonal grid receptive fields. The model proposed overcomes some crucial limitations of the current attractor and oscillatory models. It is based on the well-accepted and tested hypothesis of Hebbian learning, providing a simplified cortical-based framework that does not require the presence of theta velocity-driven oscillations (oscillatory model) or translational symmetries in the synaptic connections (attractor model). We moreover demonstrate that the proposed encoding mechanism naturally maps shifts, rotations and scaling of the stimuli onto the shape of grid cells' receptive fields, giving a straightforward explanation of the experimental evidence of grid cells remapping under transformations of environmental cues.

Author Summary

Since their discovery in 2005 grid cells have played a key-role in understanding how different species' brains dynamically represent an animal's position in space. Despite more then a decade of interest from a large number of investigators, a universally accepted model of how grid cells receptive fields emerge is still lacking. In this study we provide a new and simple theoretical and computational framework to explain how grid cells could possibly organize. We propose a novel formulation of the encoding problem through the modern Frame Theory language, providing new insights about the optimality of hexagonal grid receptive fields and overcoming some crucial limitations of the current attractor and oscillatory models. Moreover, we demonstrate that this same encoding strategy can generalize from spatial to more abstract information.

Introduction

Grid cells in the entorhinal cortex efficiently represent an animal's spatial position using an hexagonal symmetric code [1, 2]. Mathematical models have been developed to explain the emergence of such surprisingly regular firing activity [3–8]. However, the problem is far from being solved, and many questions remain open [9–12]. From the modelling point of view, two main mechanisms have been proposed to generate the hexagonal periodic activity: oscillatory interference [5] and continuous attractor dynamics [3, 4]. Let us address briefly the main ideas underlying these models.

In oscillatory models, grid cells' patterns emerge from the interference between theta oscillations of velocity-modulated cells [5, 6]. Experimental results in [13] have identified a class of cells, named band cells, that fire at specific spatial periodicity; the interference of three cells of this kind, whose wave vectors' orientations differ by multiples of 120 degrees, leads to hexagonal grid-type interference patterns. The key assumptions of oscillatory models have been experimentally challenged. Theta oscillations have not been observed in fruit bats [10] or macaque monkeys [14], despite robust grid cell activity having been recorded in both species. Furthermore, whole-cell recordings from head-fixed mice moving at different velocities, showed minimal correlation between the mouse's velocity and the amplitude or periodicity of theta oscillations [11, 15].

The core idea of continuous attractor models explains the regularity of the grid firing activity as an attractor state generated by symmetrical recurrent interactions between grid cells [3, 4]. A major weakness of this class of models is that it requires an unrealistically high degree of translational symmetry in the strength of the connections among neurons: neurons at equal distance should connect with equal strength. However, real neuronal populations are affected by noise and randomness and therefore break this symmetry and the grid regularity [9]. Alternative models based on single-cell firing, adaptation, slowly varying spatial inputs, or, more recently, on deep reinforcement learning have been proposed in [8, 16, 17]

The model we propose has at least three advantages with respect to those mentioned above. First, it is based on the well-accepted and tested hypothesis of Hebbian learning [18]. None of the complications of the interference and attractors models are needed, like the presence of theta-velocity driven oscillations or translational symmetries in the synaptic connections. Second, it naturally incorporates shifted, rotated and scaled grid cells' receptive fields remapping given transformed visual landmarks [1, 19]. Third, it gives a theoretical framework for the otherwise puzzling experimental findings in [20] where the authors show how grid cells may play a role in the organization of "conceptual" spaces. Further, it makes specific testable predictions for other experiments of the same type.

Results

Model description and predictions

The model is based on three assumptions. By analogy with the visual cortex description of Hubel and Wiesel [21, 22], we propose grid cells to emerge from a linear sum of "simple cells", whose receptive fields are learned from a collection of neuronal inputs with *stationary* second-order stimulus statistics ($\mathbf{H}1$). In other words, we assume that the encoding of the objects' movements at the level of the entorhinal cortex (the upstream neuronal responses) obeys a statistic that does not differ significantly from that of natural images (which is approximately stationary [23]). We also assume that each neuron computes a response that is the scalar product between the input and its synaptic weights i.e.

$$r_i(\mathbf{x}) = \langle \mathbf{x}, \mathbf{w}_i \rangle \tag{1}$$

with, $\mathbf{x} \in \mathbb{R}^d$ the input and $\mathbf{w}_i \in \mathbb{R}^d$ the weights of neuron i. In the following, we will fix $\mathbf{x}$ and omit to write the dependence on $\mathbf{x}$.

Furthermore, we assume that the synaptic weights are updated following Oja's rule, derived as a the first order expansion of a normalized Hebbian rule, [24], ($\mathbf{H}2$). The normalization assumption is plausible, because normalization mechanisms are widespread in the brain [25]. The original paper of Oja [26] showed that the weights of a neuron updated according to this rule will converge to the top principal component (PC) of the neuron's past input, i.e. to an eigenfunction of the input's covariance. Plausible modifications of the rule, involving added noise or inhibitory connections with similar neurons, yield additional eigenfunctions [24]. Thus, this generalized Oja's rule can be regarded as an online algorithm to compute the principal components of incoming streams of input; in our case, the stationary neuronal responses of simple cells. Our last and most important assumption is that the neural population's goal is to encode a variation of its input, in this case the position, with maximal precision [27] ($\mathbf{H}3$): neuronal responses are noisy, and thus repeated, equal stimuli can produce different outputs. ($\mathbf{H}3$) tells us that the population coding aims to minimize the variance of the responses.
The first important consequence of hypotheses ($\mathbf{H}1, \mathbf{H}2$) is that the synaptic weights of the neuronal population are tuned to Fourier functions i.e.

$$w(\mathbf{k}, \xi) = e^{I\mathbf{k}^T\xi},\ \mathbf{k}, \xi \in \mathbb{R}^2 \tag{2}$$

where I is the imaginary number and $\mathbf{k}$ is the two-dimensional frequency vector. This follows from the stationarity of neuronal input i.e. the fact that the associated covariance matrix is diagonalized by Fourier functions. A consequence of Oja's rule is that those are also the learned neuronal weights. The relative change of position of the objects in the scene (due to the animal navigating in the environment) is modelled in a first approximation as covariant translations at the level of the highly processed input of the enthorinal neurons i.e. :

$$T_{\mathbf{y}}\mathbf{x}(\xi) = \mathbf{x}(\xi - \mathbf{y}), \tag{3}$$

where $T_{\mathbf{y}}$ is the translation operator. The response of a N neurons population encoding the position of stimulus $\mathbf{y}$ will be:

$$\mathbf{r}(\mathbf{y}) = (r_1(\mathbf{y}), \cdots, r_N(\mathbf{y})) \tag{4}$$

with $r_i(\mathbf{y}) = \left\langle T_{\mathbf{y}}\mathbf{x}, e^{I\mathbf{k}_i^T\xi} \right\rangle$. The simplest model of a *"complex" grid cell* aggregates simple responses by summation:

$$r(\mathbf{y}) = \sum_{i=1}^{N} r_i(\mathbf{y}) = \left\langle T_{\mathbf{y}}\mathbf{x}, \sum_{i=1}^{N} \mathbf{w}_i \right\rangle = \sum_{i=1}^{N} c_i(\mathbf{x}) e^{I\mathbf{k}_i^T\mathbf{y}} \tag{5}$$

where $c_i(\mathbf{x})$ are the Fourier coefficients of $\mathbf{x}$ with respect to the frequencies $\mathbf{k}_i$ and $e^{I\mathbf{k}_i^T\mathbf{y}}$ are the phase factors due to the translation covariance of the Fourier transform. In general, each single simple cell's response can be considered as a random variable subject to Gaussian noise:

$$r_i(\mathbf{y}) \to r_i(\mathbf{y}) + \sigma_i. \tag{6}$$

In the following, we suppose the noise at each simple cell to be the same and uncorrelated, i.e.: $(1/\sigma^2)\mathbf{I}$. Assuming ($\mathbf{H}2$) and ($\mathbf{H}3$), the question that follows is how many neurons and which set of frequencies $\{\mathbf{k}_i\}$ are best to encode the animal's position $\mathbf{y}$ with maximal precision.

A lower bound on any possible unbiased estimator of the random variable $\mathbf{y}$ is given by the Cramer-Rao bound ([28], see Materials and Methods for more details). The bound reads:

$$\|Cov(\mathbf{y})\| \geq \left\|F^{-1}(\mathbf{y})\right\| \tag{7}$$

where $\mathbf{F}$ is the so-called *Fisher information* matrix, Cov is the covariance matrix of the neuronal responses, and $\|\cdot\|$ is a matrix norm. Intuitively, $\mathbf{F}$ measures the amount of information that the encoding population carries about the random variable $\mathbf{y}$. The main theoretical result of the paper is that the lower bound for the right hand side of Eq. 7 is achieved when the set of frequency vectors $\{\mathbf{k}_i\}$ form a so-called *Equiangular frame*. An equiangular frame is a set of vectors such that each pair of vectors form the same angle between them; i.e.

$$\mathbf{k}_p^T \mathbf{k}_q = \cos(\alpha),\ \forall\ p, q;\ \alpha \in [0, 2\pi], \alpha \text{ constant.} \tag{8}$$

We proved that the lower bound is achieved in dimension two when the number of neurons is $N = 2$, yielding the Orthonormal frame. For $N = 3$ we obtain the so-called Mercedes-Benz frame, composed by vectors whose orientations differ by 60° degrees (see Fig. 1).

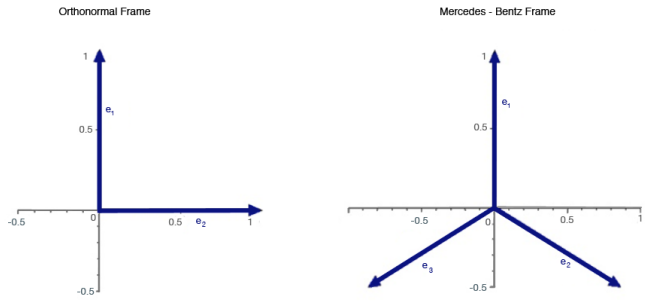


Figure 1. Orthonormal (left) and Mercedes-Benz frame (right) in dimension two. Note how the vectors in the Mercedes-Benz frame are separated by 120° one from the other.

More formally:

Theorem 1 *Given the hypotheses $H(1, 2, 3)$ the minimum variance position encoded by a set of N neurons corrupted by Gaussian uncorrelated noise is achieved when $N = 3$ and the set of frequency vectors is:*

$$f = \{\mathbf{k}_1, \mathbf{k}_2, \mathbf{k}_3\} = \{(\cos(2\pi j/3), \sin(2\pi j/3)), j = 1, \cdots, 3\}$$

or for $N = 2$ the orthonormal frame.

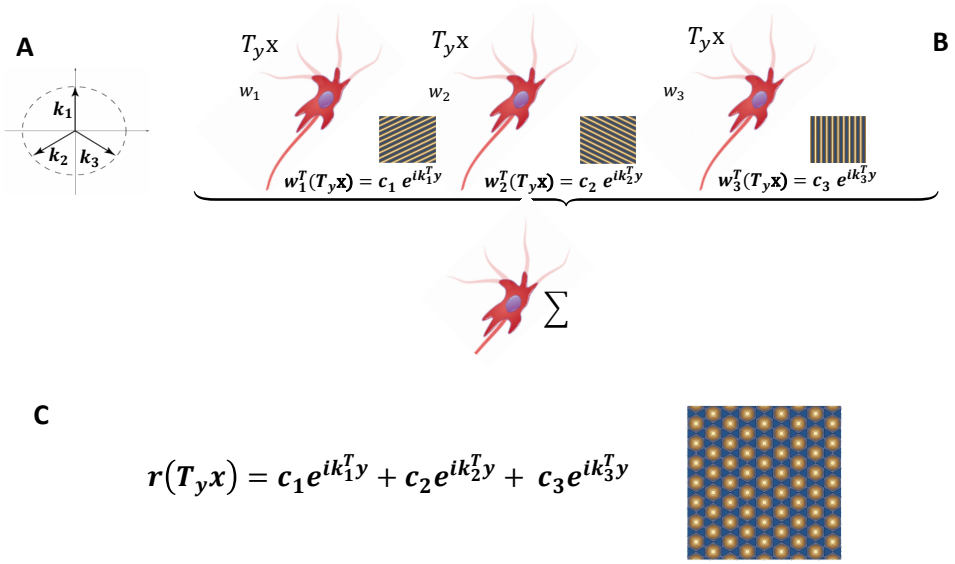


Figure 2. The figure represents how the interference of planar wave responses produces grid-like cells. (A) the Mercedes-Benz frame consisting of the equiangular vectors k_1, k_2, k_3 whose directions are along the angles $\theta = \pi/2, -\pi/6, -5\pi/6$. (B) three neurons with an input stimulus x, translated along the y vector, $T_y x$ and their receptive fields w_1, w_2, w_3, three planar waves in equiangular directions. (C) linear sum of the three neurons' responses (indicated in B as Σ) resulting in the grid-like hexagonal pattern.

The result states that the best encoding of position is achieved when the "complex" grid-like cell is aggregating the responses of two or three neurons whose neuronal weights are Fourier functions with *equiangular frequencies* in the frequency space. Suppose now the neurons' weights have been learned. The response in Eq. (5) produces output in terms of an interference pattern of two or three planar waves that is consistent with a square or hexagonal grid, respectively (see figure 2).

Importantly, the grid response is robust to arbitrary choices of the Fourier coefficients c_i (provided that none of them is zero), showing that the output grid geometry is independent of the particular input $\mathbf{x}$ (see Figure 5 in Materials and Methods).

The theoretical results described here should be compared with the biological findings in [13], where the authors find evidence for a class of cells whose spatially periodic firing patterns are composed of plane waves (or bands) drawn from a discrete set of orientations and wavelengths. Interestingly, an important subset that corresponds to three bands at $120°$ orientations is found to have the most stable firing pattern. Bands at $90°$ are also found.

2-phase application of Oja's learning rule

In the following we show how hexagonal grid receptive fileds emerges from a two-phase learning process.

First phase: "simple" cell learning. A collection of cyclical translations in the (x, y) directions of natural images is used as input stimuli to compute the "simple" cell profile of activation. Next, the principal components of these activation profiles are extracted, diagonalizing the covariance matrix of the input data. The second order statistic of the input, i.e. the covariance matrix, is clearly stationary. Note that the stationarity is independent from the nature of the stimulus and it crucially depends on the more abstract notion of transformation (in

this case translations). Under the assumption of Oja's rule, this mechanism simulates the learning phase of a "simple" cell.
An example of the learned receptive fields is shown in Fig 3 A. As expected, they are Fourier components with different directions.

Second phase: "complex" cell learning. The second step entails aggregating the responses of "simple" cells. A collection of cyclical translations of a test image is used to calculate the aggregation vector J according to the minimization problem (see Figure 3 and Materials and Methods, *Algorithmic formulation* for the algorithm details).

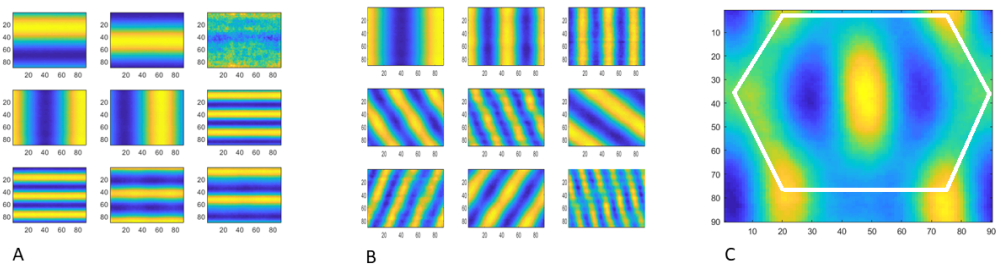


Figure 3. (A) Simple cells-like receptive fields, obtained through the first phase learning, from stationary stimuli. (B) Simple cell-like receptive fields, selected through variance minimization of the estimated position. (C) Superposition of equiangular patterns selected from figure (B), for N=3.

The results displayed in Figure 3 show that, as a result of variance minimization of the position estimate, waves with $120°$ angular distance are selected (B). Their superposition have a grid-like shape (C). Although the algorithm provides angular directions predicted by the theorem, not all superpositions produce grid-like patterns. This is due to the different frequencies of the Fourier receptive fields. For a fixed frequency, the picked receptive fields sum to produce a grid-like interference pattern. The mechanism(s) underpinning the combination of receptive fields of the same frequency is not described or included in the present algorithm and will be a direction for future work. One hypothesis that we will address is that a Foldiack type of learning may play an important role [29].

Grid remapping by changing environmental cues

Experimental evidence shows that changes in environmental cues are matched by a transformation in the animal's spatial responses [19]. This aspect can be readily explained by our model. For example, if an environmental cue is rotated by an angle θ the grid rotates accordingly, since

$$r_i(\mathbf{R}_\theta \mathbf{x}) = \langle \mathbf{R}_\theta \mathbf{x}, \mathbf{w}_i \rangle = \langle \mathbf{x}, \mathbf{R}_{-\theta} \mathbf{w}_i \rangle$$

where $\mathbf{x}$ is the input of the "simple" cell. A similar reasoning holds for scale transformations.

Discussion

We successfully showed how the hexagonal receptive fields, resembling those of grid cells, emerge naturally in the spatial encoding framework by requiring minimal variance (maximal precision) of the population encoding together with Oja's learning rule. The assumption of a 2-phase simple-complex cells type learning adapts properties typically found in the visual cortex to those characterized in the entorhinal cortex. We contend that similarity in the types of learning is plausible, given that the entorhinal cortex integrates visual information while also determining the relative position of the observer navigating the spatial environment. Importantly,

the presented model provide a theoretical framework capable of explaining the experimental evidence that grid cells encode an abstract notion of space, decoupled from the specificity of the sensory inputs. The notion indeed emerges from the mathematical group properties of the objects' transformations, rather than the objects themselves. More generally, our model would indicate that grid-like coding should manifest whenever the statistics of the neuronal inputs is stationary. Indeed, the model detailed here provides a mathematical framework able to mimic the emergence of grid-like patterns not only in a spatial encoding scheme (where the considered transformations of the space are translations), but also in a more conceptual encoding scheme (where the transformations are dilations, e.g. [20]).

Generalization of our model to "conceptual" encoding schemes

The idea that grid-like cells could provide a model to understand "cognitive", in addition to sensory-related brain functions, is not new [30, 31]. However, it was not before the work in [20] that the first experimental evidence was provided. Interestingly, our findings can be applied to outline a theoretical framework for investigating a possible computational model of their experimental evidence.

The stimuli in [20] are described in a two-dimensional *conceptual bird space*, where the position coordinates are the lengths of the neck and legs of the bird. In [20] the authors show an hexagonal grid-like pattern, while testing conceptual associations with functional magnetic resonance imaging (fMRI). For simplicity, we model the input space by using the shear group in $2D$ (composed of transformations dilating an image in the x, y directions). Instead of the ratio between the legs of the birds and their necks we can think about the ratio between the base and height of a rectangle that scale in the directions x and y, respectively, according to the parameters $(l_1, l_2) = \mathbf{l} \in \mathbb{R}^2$ (see Fig. 4, C).

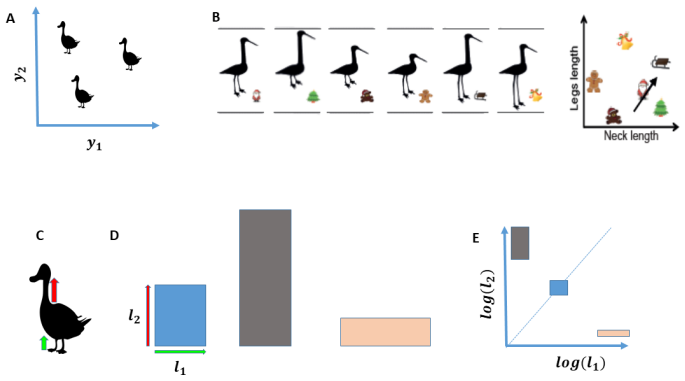


Figure 4. Translations of a bird in space (A). Transformations of a bird (B) and associated points in the 'bird space"(from [20]). Transformations of a rectangle (D) that simplify the bird transformations (C). The associated points in the "rectangle space" (E).

The transformation corresponds to Eq. (3) where instead of the translator operator the shear operator was used:

$$D_{\mathbf{l}}\mathbf{x}(\xi) = \mathbf{x}\left(\frac{\xi}{\mathbf{l}}\right). \tag{9}$$

Note that $D_{\mathbf{l}}$ indicates the shear operator. The main idea is to apply our spatial encoding to assess whether the model allows to represent the grid-like conceptual patterns observed in [20]. We stress that similarly to the bird space (where the direction of motion in the abstract "bird space" was determined by the ratio between the neck and the leg lengths), the direction of motion (in our abstract "scale space") is determined by the ratio between the base and height of the rectangle. It is simple to demonstrate that also in this case the second order statistic of the

input is stationary since it again depends only on the nature of the transformation. Therefore, the synaptic weights of the neuronal population are tuned to the eigenfunctions of the shear operator as they were before in the translation case. These eigenfunctions are a generalization of Fourier components to the shear group and have the same form, but in the log-scale coordinates $\log(\mathbf{l}) = (log(l_1), log(l_2))$, where l_1, l_2 are the scaling factors in the x and y directions (see e.g. [32]) :

$$s(\mathbf{l}, \mathbf{k}) = e^{I\mathbf{k}^T \log(\mathbf{l})}. \tag{10}$$

The key observation is that in this new coordinate frame (provided by the response of the "simple cells") shear transformations reduce to translations in the $\log(\mathbf{l})$-space since:

$$\log(\mathbf{l}\mathbf{l}') = \log(\mathbf{l}) \log(\mathbf{l}'). \tag{11}$$

In this space the eigenfunctions are planar waves as in Fig. 2 A, applying Theorem 1. We can then prove that also in this case the set of frequency vectors $\{\mathbf{k}_i\}$ is the Mercedes-Benz frame or the orthonormal frame. This will produce a square or hexagonal grid in the *shear space*, where the coordinates are the scale parameters $\mathbf{l}$ i.e. in the rectangle-space illustrated in Fig. 4, (E).

The results in Theorem 1 can be generalized to any Abelian group; the eigenfunctions of the group transformations are the group characters [32]. It can be used to predict grid-like cell geometries in higher dimensions. In dimension three, a possible solution corresponds to the vectors associated to the vertices of a tetrahedron. More generally, in dimension d we will end up with the vectors associated to the vertices of a Platonic Solid. However, it should be noted that many other solution configurations might exist that are distinct from the case of $d = 2$ analyzed in this paper.

Conclusion and Outlook

We detailed a computational model able to account for the emergence of hexagonal grid-like response patterns that derives from neural sensitivity to the statistics of the input stimuli (i.e. minimal variance encoding). By applying Frame Theory, we provided a novel formulation of the encoding problem, specifically that of equiangular Frames. Our model overcomes limitations described for both oscillatory and attractor models. Moreover, we were able to demonstrate that grid-like receptive field patterns persist despite transformations of the environmental cues as well as when more "conceptual" features are input. Further work will be required to extend our findings to reproduce the experimental evidence showing that the regular pattern of the grid receptive field adapts to different geometries of the environment, distorting its hexagonal regularity [33, 34]. Furthermore, our main result in Theorem 1 predicts the same hexagonal grid for the 3D space of rotations of an object, leading to a series of experiments in the same spirit of [35–37] (for spatial encoding) and of [20] for conceptual encoding.

Materials and Methods

Fisher information

The Cramer-Rao bound (CRB) sets a lower bound on the norm of the covariance operator of any random variable unbiased estimator. It says:

$$\|Cov(\mathbf{y})\| \leq \left\|F^{-1}(\mathbf{y})\right\|$$

where $\mathbf{y}$ is our position variable, F is the Fisher information defined as:

$$(F(\mathbf{y}))_{k,l} = -\mathbb{E}\Big(\frac{\partial^2 \log L(\mathbf{y})}{\partial y_k \partial y_l}\Big)$$

and $L(\mathbf{y})$ is the likelihood function and the average is over of the measurements of $\mathbf{y}$. In our case the likelihood function is, [38]:

$$L(\mathbf{y}) = \mathcal{N} exp\Big(-\frac{1}{2}\sum_{i,j=1}^{N}(y_i - r_i(\mathbf{y}))C_{ij}^{-1}(y_j - r_j(\mathbf{y}))\Big). \tag{12}$$

where $\mathcal{N}$ is a normalization constant, C is the correlation matrix of the Gaussian noise and r_i is the response of the i^{th} neuron. Under the hypothesis of uncorrelated equal noise, i.e. $\mathbf{C} = (1/\sigma^2)\mathbf{I}$, a direct calculation of Eq. (12) gives:

$$\mathbf{F}(\mathbf{y}) \quad = \quad -\mathbb{E}\Big\{\Big(\frac{\partial \mathbf{r}(\mathbf{y})}{\partial \mathbf{y}}\Big)^{\dagger}\mathbf{C}\frac{\partial \mathbf{r}(\mathbf{y})}{\partial \mathbf{y}}\Big\} = -\frac{1}{\sigma^2}\mathbb{E}\Big\{\Big(\frac{\partial \mathcal{F}(T_{\mathbf{y}}\mathbf{x})}{\partial \mathbf{y}}\Big)^{\dagger}\frac{\partial \mathcal{F}(T_{\mathbf{y}}\mathbf{x})}{\partial \mathbf{y}}\Big\},$$

where $\mathcal{F}$ is the Fourier transform. Starting from the following identity:

$$\frac{\partial \mathcal{F}_i(T_{\mathbf{y}}\mathbf{x})}{\partial \mathbf{y}} = Ie^{I\mathbf{k}_i{}^T\mathbf{y}}\mathbf{k}_i c_i(\mathbf{x}), \;\; \mathbf{c}(\mathbf{x}) = \mathcal{F}(\mathbf{x}), \tag{13}$$

we have:

$$\begin{aligned}\mathbf{F} \quad &= \quad \frac{1}{\sigma^2}\mathbb{E}\Big\{\sum_{i=1}^{N}\mathbf{k}_i\mathbf{k}_i{}^T|c_i(\mathbf{x})|^2\Big\}\frac{1}{\sigma^2}\sum_{i=1}^{N}\mathbf{k}_i\mathbf{k}_i{}^T\mathbb{E}(|c_i(\mathbf{x})|^2) \\ &= \quad \frac{1}{\sigma^2}\sum_{i=1}^{N}\frac{\mathbf{k}_i\mathbf{k}_i{}^T}{\|\mathbf{k}_i\|_2^2} = \frac{1}{\sigma^2}\sum_{i=1}^{N}\mathbf{g}_i\mathbf{g}_i{}^T\end{aligned} \tag{14}$$

where we used the fact that the averaged power spectrum $\mathbb{E}(|c_i(\mathbf{x})|^2) \approx \|\mathbf{k}_i\|_2^{-2}$ and we define the unit norm vector $\mathbf{g}_i = \mathbf{k}_i/\|\mathbf{k}_i\|$.
The question we address in the next paragraph is: for which set of $\mathbf{k}_i$ is the (CRB) achieved? In other words, we are looking for the values of $\mathbf{k}_i$ for which the neuronal population is providing an estimate of the variable $\mathbf{y}$ with minimal variance. In particular we consider the following minimization problem:

$$\underset{\{\mathbf{k}_i\}}{\operatorname{argmin}} \left\|\mathbf{F}^{-1}\right\|_{Frob}^2. \tag{15}$$

Optimal estimator and connection with frame theory

In this section we derive the proof of the main result of the paper:

Theorem 2 *Under the hypotheses* $\mathbf{H}(1,2,3)$ *the minimal variance position encoded by a set of* N *neurons corrupted by Gaussian uncorrelated noise is achieved when* $N = 3$ *and the set of frequency vectors is:*

$$f = \{\mathbf{k}_1, \mathbf{k}_2, \mathbf{k}_3\} = \{(cos(2\pi j/3), sin(2\pi j/3)), j = 1, \cdots, 3\}.$$

or when $N = 2$ *for the set of frequencies forms an orthonormal frame.*

Proof 1 *Using the fact that* $\mathbf{F}$ *is semi-positive definite we can decompose it as* $\mathbf{F} = \mathbf{V}^T\mathbf{\Lambda}\mathbf{V}$ *where* $\mathbf{V}$ *is unitary and* $\mathbf{\Lambda}$ *is diagonal. According to the Cramer-Rao bound the variance is bounded from below by the inverse of the Fisher Information. Calculating the Frobenius norm of the Fisher matrix inverse we have:*

$$\left\|\mathbf{F}^{-1}\right\|^2 = Tr(\mathbf{V}^T(\mathbf{\Lambda}^{-1})^2\mathbf{V}) = Tr((\mathbf{\Lambda}^{-1})^2) = \sum_{i=1}^{N}\frac{1}{\lambda_i^2} \tag{16}$$

where λ_i are the eigenvalues of $\mathbf{F}$.
It is easy to prove that the minimum of eq.(16) *is reached when all the eigenvalues are equal i.e.*

$$\mathbf{F} = \lambda \mathbf{I} \tag{17}$$

i.e. the set $\mathbf{k_i}$ form a tight frame. When N is equal to $2, 3$, the only solutions are (see [39], pg 210): for $N = 2$, the orthogonal frame, for $N = 3$ the so called Mercedes-Benz frame (or any rotated version of them):

$$\mathbf{k}_j = \Big(\cos(\frac{2\pi j}{3}), \sin(\frac{2\pi j}{3}) \Big) \quad j = 1, \cdots, 3.$$

Remark 1 *In the three dimensional case a similar result still holds: a possible solution corresponds to the vectors associated to the vertices of a tetrahedron. More in general in dimension d will be the vectors associated to the vertices of a Platonic Solid. However the uniqueness of the solution is guaranteed only in dimension two.*

Algorithmic formulation

In this article we suppose a 2-phases learning process:

(1) Learning of the Fourier components by simple cells using Oja's synaptic updating rule;

(2) Learning of the selection of simple cells, performed by the complex cell that minimize, according to the Cramer-Rao bound, the norm of the inverse of the Fisher Information.

Solving phase 1 simply correspond to the extraction of the principal components of neural input. As for phase 2 the minimization problem for the complex cell is:

$$\underset{\{\mathbf{k_i}\}_{i=1}^{N}}{\operatorname{argmin}} \quad \left\| F^{-1} \right\|^2 \quad \text{with} \quad N \quad \text{minimal.} \tag{18}$$

As we saw in Eq. (14), the minimization of $\left\| F^{-1} \right\|^2$ is achieved when the set $\{\mathbf{g}_i\}$ forms a tight frame. Tight frames are minima of the so called *frame potential* (see [40]), calculated as:

$$FP(\{\mathbf{g}_i\}) = \sum_{ij=1}^{N} |\mathbf{g}_i^T \mathbf{g}_j|^2. \tag{19}$$

Let us calculate the frame potential in our case. Here we denote with W the matrix whose columns are the vectors $\mathbf{w}_i$, simple cells receptive fields. Hence the response matrix (i.e. the simple cells output) will be $A = X^T W$ where X is the dataset corresponding to the initial stimuli. The complex grid cells will then aggregate some of the responses, i.e. they will calculate AJ where J is a vector of zeros and ones selecting which simple cells are meant to aggregate (we will have a zero whether the simple cell is not selected in the aggregation process and one elsewhere). We can now use this notation to write the Fisher information as follows:

$$F = -\Big(\frac{\partial \mathbf{r}(\mathbf{y})}{\partial \mathbf{y}} \Big)^{\dagger} \frac{\partial \mathbf{r}(\mathbf{y})}{\partial \mathbf{y}} = J^T \dot{A}^T \dot{A} J = J^T R J. \tag{20}$$

with the dot indicating the derivative and $R = \dot{A}^T \dot{A}$. In order to minimize the number of simple cells pooled by the complex cell, we add a sparsifying term in $\|J\|_0$ or its relaxation $\|J\|_1$.

Gradient descent: Given the above reasoning our minimization problem boils down to:

$$\underset{J}{\operatorname{argmin}} \quad \left\| J^T R J \right\|^2 + \lambda \left\| J \right\|_1 \tag{21}$$

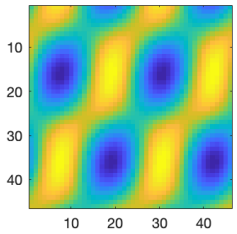
To find the solution we adopt a gradient descent strategy with shrinkage: A simple calculation shows that the update rule for J is:

$$J \to thr(J - \lambda \, RJJ^T RJ) \tag{22}$$

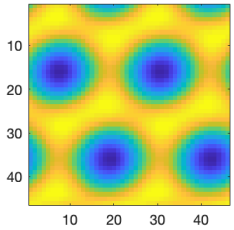
where the thr threshold is enforcing the sparsity constraint.

Grid geometry is input independent

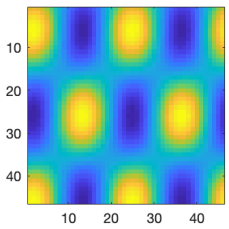
As mentioned in the main text, the receptive field shape of the grid cells is robust to different choices of the Fourier coefficients.



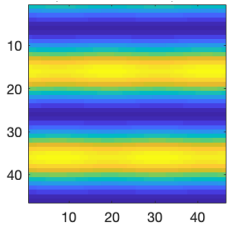
(a) First interference grid pattern, with $c_1 = -0.19$, $c_2 = -0.84$, $c_3 = -0.52$.



(b) Second interference grid pattern, with $c_1 = -0.75$, $c_2 = -0.63$, $c_3 = -0.52$.



(c) Third interference grid pattern, with $c_1 = -0.17$, $c_2 = -0.9$, $c_3 = 0.8$.



(d) Fourth interference grid pattern, with $c_1 = 0.88$, $c_2 = -0.01$, $c_3 = -0.02$. Here two coefficients are degenerate.

Figure 5. Interference of planar waves modulated by random c_i, $i \in \{1, 2, 3\}$ Fourier coefficients. The grid geometry is independent from the particular input x (a-c). Only in very highly improbable cases when one of the coefficients is zero the grid shape fails to appear (d).

Acknowledgements

M.M.M. is supported by grants from the Swiss National Science Foundation (grant 320030-169206), the Fondation Asile des Aveugles, and a grantor advised by Carigest. B.F. is supported by the Fondation Asile des Aveugles. L. R. and F.A. acknowledges the financial support of the AFOSR projects FA9550-17-1-0390 and BAA-AFRL-AFOSR-2016-0007 (European Office of Aerospace Research and Development), and the EU H2020-MSCA-RISE project NoMADS - DLV-777826. This material is based upon work supported by the Center for Brains, Minds and Machines (CBMM), funded by NSF STC award CCF-1231216, and the Italian Institute of Technology.

References and Notes

1. Hafting T, Fyhn M, Molden S, Moser MB, Moser EI. Microstructure of a spatial map in the entorhinal cortex. Nature. 2005;436:801–806.
2. Burak Y, Fiete IR. Accurate path integration in continuous attractor network models of grid cells. PLoS Comput Biol. 2009;5.
3. McNaughton BL, Battaglia FP, Jensen O, Moser EI, Moser MB. Path integration and the neural basis of the 'cognitive map'. Nature Rev Neurosci. 2006;7:663–678.
4. Fuhs MC, Touretzky DS. A spin glass model of path integration in rat medial entorhinal cortex. J Neurosci. 2006;6:4266–4276.
5. Burgess N, Barry C, O'Keefe J. An oscillatory interference model of grid cell firing. Hippocampus. 2007;17:801–812.
6. Hasselmo ME, Giocomo LM, Zilli EA. Grid cell firing may arise from interference of theta frequency membrane potential oscillations in single neurons. Hippocampus. 2007;17:1252–1271.
7. Blair HT, Welday AC, Zhang K. Scale-invariant memory representations emerge from moire interference between grid fields that produce theta oscillations: a computational model. J Neurosci. 2007;27:3211–3229.
8. Kropff E, Treves A. The emergence of grid cells: intelligent design or just adaptation? Hippocampus. 2008;18:1256–1269.
9. Renart A, Song P, Wang XJ. Robust spatial working memory through homeostatic synaptic scaling in heterogeneous cortical networks. Neuron. 2003;38:473–485.
10. Yartsev MM, Witter MP, Ulanovsky N. Grid cells without theta oscillations in the entorhinal cortex of bats. Nature. 2011;479:103–107.
11. Schmidt-Hieber C, Häusser M. Cellular mechanisms of spatial navigation in the medial entorhinal cortex. Nature Neurosci. 2013;16:325–331.
12. Heys JG, MacLeod KM, Moss CF, Hasselmo ME. Bat and rat neurons differ in theta frequency resonance despite similar coding of space. Science. 2013;340:363–367.
13. Krupic J, Burgess N, O'Keefe J. Neural Representations of Location Composed of Spatially Periodic Bands. Science, Aug 2012: Vol 337, Issue 6096, pp 853-857. 2012;.
14. Killian NJ, Jutras MJ, Buffalo EA. A map of visual space in the primate entorhinal cortex. Nature. 2012;491:761–764.

15. Domnisoru C, Kinkhabwala AA, W TD. Membrane potential dynamics of grid cells. Nature. 2013;495:199–204.

16. Franzius M, Sprekeler H, Wiskott L. Slowness and Sparseness Lead to Place, Head-Direction, and Spatial-View Cells. Plos Computational Biology. 2007;3(8):1605–1622.

17. Banino A, Barry C, Uria B, Blundell C, Lillicrap T, Mirowski P, et al. Vector-based navigation using grid-like representations in artificial agents. Nature. 2018;557. doi:10.1038/s41586-018-0102-6.

18. Hebb DO. The organization of behavior: A neuropsychological theory. Wiley; 1949.

19. Fyhn M, Hafting T, Treves A, Moser M, Moser E. Hippocampal remapping and grid realignment in entorhinal cortex. Nature. 2007;446:190–194.

20. Constantinescu AO, O'Reilly JX, Behrens TEJ. Organizing conceptual knowledge in humans with a gridlike code. Science Vol 352, pp 1464-1468. 2016;.

21. Hubel D, Wiesel T. Receptive fields and functional architecture in two nonstriate visual areas (18 and 19) of the cat. Journal of Neurophysiology. 1965;28(2):229.

22. Hubel D, Wiesel T. Receptive fields and functional architecture of monkey striate cortex. The Journal of Physiology. 1968;195(1):215.

23. DJ F. Wavelets, Vision and the Statistics of Natural Scenes. Philosophical Transactions: Mathematical, Physical and Engineering Sciences. 1999;357(1760):2527.

24. Oja E. Principal components, minor components, and linear neural networks. Neural Networks. 1992;5(6):927–935.

25. Carandini M, Heeger DJ. Normalization as a canonical neural computation. . . . Nat Rev Neurosci. 2011;13(1):51–62.

26. Oja E. Simplified neuron model as a principal component analyzer. Journal of Mathematical Biology. 1982;15(3):267–273.

27. S D, E P, Latham, Alexandre P. Reading population codes: a neural implementation of ideal observers. Nature Neuroscience. 1999;2(8):740–745.

28. M KS. Fundamentals of statistical signal processing: Estimation theory. New Jersey: Englewood Cliffs; 1993.

29. Földiák P. Learning invariance from transformation sequences. Neural Computation. 1991;3(2):194–200.

30. Moser EI, Moser MB. Grid Cells and Neural Coding in High-End Cortices. Neuron. 2013;80.

31. Moser EI, Roudi Y, Witter MP, Kentros C, Bonhoeffer T, Moser MB. Grid cells and cortical representation. Nature Reviews Neuroscience. 2014;15:466–481.

32. Eagleson R. Measurement of the 2D affine Lie group parameters for visual motion analysis. . . . Spatial Vision. 1992;6,3.

33. Krupic J, Bauza M, Burton S, Lever C, O'Keefe J. How environment geometry affects grid cell symmetry and what we can learn from it. . . . Philos Trans R Soc Lond B Biol Sci. 2014;369.

34. Urdapilleta E, Troiani F, Stella F, Treves A. Can rodents conceive hyperbolic spaces? Journal of the Royal Society Interface. 2015;12, 107.

35. Cheng D. Hexadirectional Modulation of Theta Power in Human Entorhinal Cortex during Spatial Navigation. Current Biology. 2018;28:20:3310–3315.

36. Kim M. Can we study 3D grid codes non-invasively in the human brain? Methodological considerations and fMRI findings. NeuroImage. 2019;186:667–678.

37. Jacobs J. Direct recordings of grid-like neuronal activity in human spatial navigation. Nature Neuroscience. 2013;16:1188–1190.

38. Yoon H, Sompolinsky H. The Effect of Correlations on the Fisher Information of Population Codes. In: Proceedings of the 11th International Conference on Neural Information Processing Systems. NIPS 98. Cambridge, MA, USA: MIT Press; 1998. p. 167–173.

39. Goyal VK, Kovacevic J. Quantized Frame Expansions with Erasures. Applied and Computational Harmonic Analysis. 2001;10:203–233.

40. Casazza G P, Fickus M, Kovačević J, Leon T M, Tremain C J. A Physical Interpretation of Tight Frames. . . . Harmonic Analysis and Applications Applied and Numerical Harmonic Analysis. 2006;.